On the steady-state chemical potential profiles in bilayer solid electrolytes

Han-Ill Yoo,[a] Tae-Hyun Kwon,[b] and Taewon Lee
WCU Hybrid Materials Program, Department of Materials Science and Engineering, Seoul National University, Seoul 151-744, Korea

(Received 10 January 2012; accepted 1 June 2012)

All the existing theories presuppose the continuity of oxygen chemical potential at interfaces between contiguous layers, in calculating steady-state chemical potential profiles across a multilayer composite of mixed conductor oxides that is subjected to an oxygen chemical potential gradient of whatsoever origin, but they have never been tested experimentally. We have observed that this continuity hypothesis appears to break down in yttria-stabilized zirconia/gadolinia-doped ceria bilayer electrolytes under an electric tension in ion-blocking condition (Hebb–Wagner polarization). It is suggested that all the continuity hypothesis-based existing theories to calculate the steady-state chemical potential distributions may not always be true depending on boundary conditions.

I. INTRODUCTION

It has long been of fundamental as well as practical interest to calculate or predict oxygen chemical potential profiles in a single-layer or multilayer composite of mixed conductor oxides under various boundary conditions.[1–8] Particularly for bilayer electrolytes involving a main electrolyte with superior ionic conductivity but with too poor thermodynamic stability or too narrow electrolytic domain, and a complementary electrolyte with inferior ionic conductivity but with superior thermodynamic or electrolytic stability, e.g., $Ce_{1-x}Gd_xO_{2-x/2}$ (GDC)/$Zr_{1-x}Y_xO_{2-x/2}$ (YSZ) and $Bi_{2-x}Y_xO_{3-x/2}$ (YSB)/YSZ, oxygen chemical potential distribution is practically very important to ensure the thermodynamic or electrolytic stability of easily reducible GDC or easily decomposable YSB under solid oxide fuel cell conditions.[1–5]

It was Wagner[9] who first tried to calculate the steady-state distribution of chemical potentials across heterogeneous phases. He was concerned with the open-circuit voltage E of the galvanic cell:

$$\mathrm{Ag|AgI|Ag_2S|Pt(+S)} \quad . \tag{1}$$

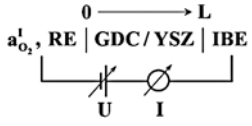
The open-circuit voltage is determined by the distribution of Ag chemical potential (μ_{Ag}) in the cell. In his calculation,[9] he tacitly hypothesized that the distribution will be continuous at the interface between AgI and Ag_2S and assigned a common chemical potential value μ'_{Ag}. Later on, authors[1–6] continued to adopt the same continuity hypothesis in dealing with the chemical potential distribution in a multilayer assembly subjected to a chemical potential difference of whatsoever origin. This continuity hypothesis is now widely accepted with little doubt, but it has never been tested experimentally.

We have recently measured the electronic conductivity of bilayer $Ce_{0.9}Gd_{0.1}O_{1.95}$ (GDC)/$Zr_{0.84}Y_{0.16}O_{1.92}$ (YSZ) electrolytes by using the Hebb–Wagner polarization method.[10] In this course of work, we have observed that the continuity hypothesis appears to break down. The consequence would not be trivial: all the existing theories based on this hypothesis may not always be true.

We will hereby report on the possible failure of the hypothesis in detail by presenting the as-measured current (I) versus voltage (U) and electronic conductivity (σ_e), thereby calculating these on the basis of the continuity hypothesis and comparing each other. The failure strongly suggests that there may have to be a discontinuity of oxygen potential at an interface between two contiguous electrolytes. We will subsequently calculate this interfacial potential drop to compare with the overall drop across the entire GDC/YSZ bilayer.

II. I VERSUS U AND σ_e AS MEASURED

Let us consider a Hebb–Wagner polarization cell involving a bilayer electrolyte GDC/YSZ with the common cross section "A" and thickness of L_C and L_Z, respectively:



, (2)

where RE and IBE denote the reversible and ion-blocking electrode, respectively, and $a^I_{O_2}$ the oxygen activity fixed at RE. When a current I is driven toward IBE by a dc voltage U applied relative to IBE, the oxygen chemical potential at

[a]Address all correspondence to this author.
e-mail: hiyoo@snu.ac.kr
[b]Present address: Battery Tech Center, LG Chemical Research Park, Daejeon, Korea
DOI: 10.1557/jmr.2012.201

 © Materials Research Society 2012

https://doi.org/10.1557/jmr.2012.201 Published online by Cambridge University Press

the right end of the bilayer ($x = L = L_C + L_Z$) in contact with IBE, μ_O^{II}, or oxygen activity there, $a_{O_2}^{II}$, is lowered relative to the left end ($x = 0$) as:

$$\mu_O^{II} - \mu_O^{I} = \frac{1}{2}RT\ln\frac{a_{O_2}^{II}}{a_{O_2}^{I}} = -2(\eta_e^{II} - \eta_e^{I}) = -2FU \quad , \quad (3)$$

because $\nabla\,\eta_i = \nabla\,\mu_O + 2\nabla\,\eta_e = 0$ in steady state, where η_k stands for the electrochemical potential of oxide ions (k = i) and electrons (k = e).

Letting σ_e denote the partial electronic conductivity of the bilayer as a whole, the steady-state current, which is totally electronic, is given as

$$i = \frac{I}{A} = \frac{\sigma_e}{F}\nabla\eta_e \quad , \quad (4a)$$

which may be rewritten, due to Eq. (3), as:

$$\frac{I}{A} = -\frac{\sigma_e}{2F}\nabla\mu_O = -\frac{RT\sigma_e}{4F}\nabla\ln a_{O_2} \quad . \quad (4b)$$

Upon integration along the length L, one obtains

$$\frac{IL}{A} = -\frac{1}{2F}\int_{\mu_O^I}^{\mu_O^{II}}\sigma_e d\mu_O \quad . \quad (5)$$

The electronic conductivity at μ_O^{II}, $\sigma_e(\mu_O^{II})$, of the bilayer as a whole can, thus, be determined from the instantaneous slopes of I versus U as measured with μ_O^I or $a_{O_2}^I$ fixed or

$$\sigma_e(\mu_O^{II}) = -2F\frac{L}{A}\left(\frac{\partial I}{\partial\mu_O^{II}}\right)_{\mu_O^I} = \frac{L}{A}\left(\frac{\partial I}{\partial U}\right)_{\mu_O^I} \quad . \quad (6)$$

Experimental details are already given elsewhere.[10] Briefly, the bilayers used were prepared by pulsed laser depositing YSZ films onto GDC disks as the main electrolytes. As IBE, Pt was first coated upon the as-deposited YSZ to a thickness of ~1 μm, and then upon it, a Pt foil of 100 μm thickness was attached with the aid of Pt paste. As RE, a Pt net (100 mesh) was attached onto the other surface of the bilayer by lightly applying Pt paste. To secure firm attachment of these electrodes, the bilayer electrolyte as such was subsequently fired at ~1000 °C under a light spring pressure, and the lateral surface of each cell was completely sealed with a glass. The steady-state voltage U across the cell was monitored relative to IBE, while passing a constant current I from RE to IBE.

I versus U as measured on the $Ce_{0.9}Gd_{0.1}O_{1.95}$/$Zr_{0.84}Y_{0.16}O_{1.92}$ bilayer of L_C = 1 mm and L_Z = 1 μm with $a_{O_2}^I = 0.21$ at 800, 900, and 1000 °C, respectively, are shown (solid circles) in Fig. 1, and σ_e thereby due to Eq. (6) is shown (symbols) in Fig. 2.

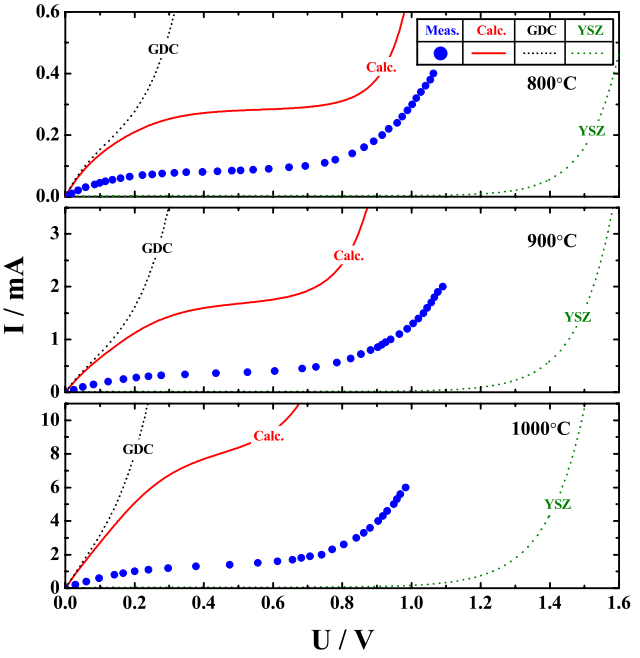


FIG. 1. I versus U as measured (solid circles) on the $Ce_{0.9}Gd_{0.1}O_{1.95}/Zr_{0.84}Y_{0.16}O_{1.92}$ bilayer electrolyte of thickness ratio of L_C/L_Z = 1 mm/1 μm by Hebb–Wagner polarization method and as calculated for the bilayer (solid lines) as well as both end-member electrolytes (dotted lines) at 800 °C (top), 900 °C (middle), and 1000 °C (bottom), respectively, with air as the reference oxygen activity ($a_{O_2}^I$ = 0.21).

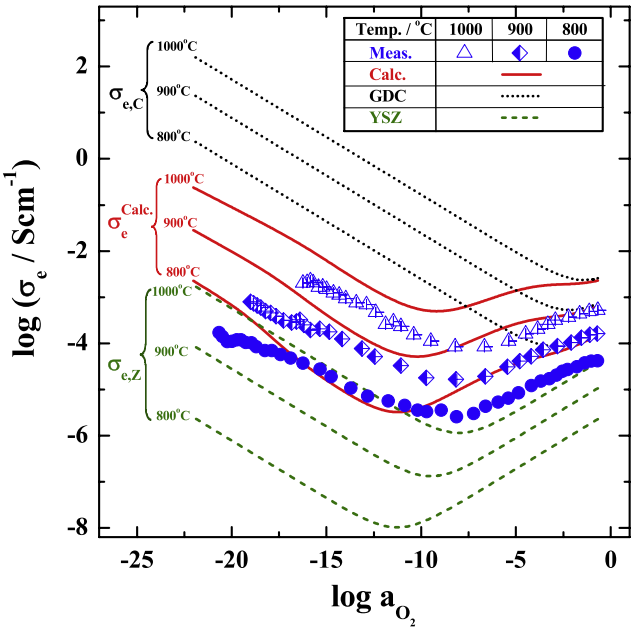


FIG. 2. Electronic conductivity versus oxygen activity of $Ce_{0.9}Gd_{0.1}O_{1.95}/Zr_{0.84}Y_{0.16}O_{1.92}$ bilayer as measured (symbols) and as calculated (solid lines) at three different temperatures. For comparison, the as-calculated electronic conductivities of both end-member electrolytes are given (dotted lines).

https://doi.org/10.1557/jmr.2012.201 Published online by Cambridge University Press

III. *I* VERSUS *U* AND σ_e AS CALCULATED ON THE BASIS OF THE CONTINUITY HYPOTHESIS

Equation (5) indicates that once σ_e is known as a function of μ_O (= $\mu_{O_2}/2$) or a_{O_2}, one can execute integration to eventually obtain I versus U due to Eq. (3). The partial electronic conductivity is known as[11–13]

$$\sigma_{e,\phi} = \sigma^*_{n,\phi}\left(\frac{a_{O_2}}{a^*_{O_2}}\right)^{-1/4} + \sigma^*_{p,\phi}\left(\frac{a_{O_2}}{a^*_{O_2}}\right)^{+1/4} \quad , \qquad (7)$$

for each end-member electrolyte ϕ of the bilayer within its electrolytic domain, where $\sigma^*_{n,\phi}$ and $\sigma^*_{p,\phi}$ denote the conductivity by electrons and holes of the electrolyte ϕ, respectively, at the reference oxygen activity $a^*_{O_2}$. One thus obtains the I versus U for the electrolyte ϕ with thickness L_ϕ as

$$I = \frac{ART}{L_\phi F}\left\{\sigma^*_{n,\phi}\left[\exp\left(\frac{FU}{RT}\right) - 1\right] + \sigma^*_{p,\phi}\left[1 - \exp\left(-\frac{FU}{RT}\right)\right]\right\} \quad , \qquad (8)$$

when $a^*_{O_2} = a^I_{O_2}$.

For the end-member electrolytes YSZ (ϕ = Z) and GDC (ϕ = C), the reference conductivities $\sigma^*_{n,\phi}$ and $\sigma^*_{p,\phi}$ at $a^*_{O_2}$ = 0.21 take the numerical values as given in Table I. Using these values, we calculated, via Eq. (8), the I versus U for each end-member electrolyte YSZ and GDC with L_ϕ = L (=1 mm + 100 nm) at the three different temperatures, which are shown (dotted lines) in Fig. 1. The partial electronic conductivity as given in Eq. (7) or equivalently as calculated back via Eq. (6) from Eq. (8) is plotted (dotted lines) for each end-member electrolyte at the three corresponding temperatures in Fig. 2.

Let us now calculate the electronic conductivity of the bilayer itself by using the continuity hypothesis. The hypothesis stipulates a single value of oxygen chemical potential, μ^i_O, at the GDC/YSZ interface, see Fig. 3(a). Once the steady state is achieved in Cell (2), the current I, which is now totally electronic, should be rendered constant and continuous across the two electrolyte phases or

$$I = I_c = I_z \quad . \qquad (9)$$

Due to Eq. (5), thus, one has

$$\frac{I}{A} = -\frac{1}{2FL_C}\int_{\mu^I_O}^{\mu^i_O}\sigma_{e,C}\,d\mu_O = -\frac{1}{2FL_Z}\int_{\mu^i_O}^{\mu^{II}_O}\sigma_{e,Z}\,d\mu_O \quad , \qquad (10)$$

which is subsequently integrated, by using Eq. (7), to

$$\frac{FI}{ART} = \frac{1}{L_C}\left\{\sigma^*_{n,C}\left[1 - \left(\frac{a^i_{O_2}}{a^*_{O_2}}\right)^{-1/4}\right] + \sigma^*_{p,C}\left[\left(\frac{a^i_{O_2}}{a^*_{O_2}}\right)^{+1/4} - 1\right]\right\} \quad , \qquad (11a)$$

$$\frac{FI}{ART} = \frac{1}{L_Z}\left\{\sigma^*_{n,Z}\left[\left(\frac{a^i_{O_2}}{a^*_{O_2}}\right)^{-1/4} - \left(\frac{a^{II}_{O_2}}{a^*_{O_2}}\right)^{-1/4}\right] + \sigma^*_{p,Z}\left[\left(\frac{a^{II}_{O_2}}{a^*_{O_2}}\right)^{+1/4} - \left(\frac{a^i_{O_2}}{a^*_{O_2}}\right)^{+1/4}\right]\right\} \quad , \qquad (11b)$$

for the experimental condition $a^I_{O_2} = a^*_{O_2}$. These simultaneous equations can be analytically solved for $(a^i_{O_2}/a^*_{O_2})^{-1/4}$ in terms of $a^{II}_{O_2}$ and materials parameters $\sigma^*_{n,\phi}$ and $\sigma^*_{p,\phi}$. By substituting the solution back into Eqs. (11a) or (11b) one obtains the analytic equation for I versus U with the aid of Eq. (3) as

$$I = \frac{ART}{F}\left\{P_3 e^{FU/RT} - P_3\left[\frac{2(P_1+P_2)}{g(U)+h(U)}\right] - P_1 e^{-FU/RT} + P_1\left[\frac{2(P_1+P_2)}{g(U)+h(U)}\right]^{-1}\right\} \quad , \qquad (12)$$

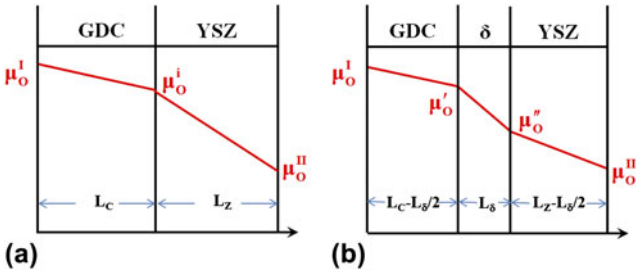


FIG. 3. Oxygen chemical potential distribution across a bilayer YSZ/GDC electrolyte (a) in the conventional picture and (b) in a newly proposed picture. Note an extra potential drop across an interphase δ with a thickness L_δ such that $L_\delta \ll L_C, L_Z$.

TABLE I. Numerical values for the electron and hole conductivities at the reference state $a^*_{O_2}$= 0.21, from Refs. 11–13.

	YSZ (ϕ = Z)[11]			GDC (ϕ = C)[12,13]		
	800 °C	900 °C	1000 °C	800 °C	900 °C	1000 °C
$\sigma^*_{n,\phi}$ (S/cm)	1.16×10^{-11}	4.15×10^{-10}	8.46×10^{-9}	1.16×10^{-5}	1.14×10^{-4}	7.81×10^{-4}
$\sigma^*_{p,\phi}$ (S/cm)	2.28×10^{-6}	1.06×10^{-5}	3.90×10^{-5}	1.70×10^{-4}	4.76×10^{-4}	1.88×10^{-3}

https://doi.org/10.1557/jmr.2012.201 Published online by Cambridge University Press

and according to Eq. (6), the conductivity of the bilayer as a whole as

$$\sigma_e(a''_{O_2}) = Lf(U)\left\{1 - \frac{P_1}{2(P_1+P_2)}\left[1 + g(U)/h(U)\right] - 2P_3(P_1+P_2)\frac{[1+g(U)/h(U)]}{[g(U)+h(U)]^2}\right\} \quad , \quad (13)$$

where

$$P_1 \equiv \frac{\sigma^*_{p,Z}}{L_Z};\ P_2 \equiv \frac{\sigma^*_{p,C}}{L_C};\ P_3 \equiv \frac{\sigma^*_{n,Z}}{L_Z};\ P_4 \equiv \frac{\sigma^*_{n,C}}{L_C};$$

$$f(U) \equiv P_1 e^{-FU/RT} + P_3 e^{FU/RT};$$

$$g(U) \equiv P_1 e^{-FU/RT} + P_2 - P_3 e^{FU/RT} - P_4;$$

$$h(U) \equiv \sqrt{g(U)^2 + 4(P_1+P_2)(P_3+P_4)} \quad .$$

Using the materials parameters in Table I, I versus U [Eq. (12)] is plotted (solid lines) at the three temperatures in Fig. 1, and σ_e versus $\log a''_{O_2}$ [Eq. (13)] in Fig. 2.

In Figs. 1 and 2, one can clearly see that as expected, I versus U as well as σ_e versus $\log a''_{O_2}$ of the GDC/YSZ bilayer, whether calculated or measured, are all bounded by the calculated ones of the end-member electrolytes, but for the bilayer itself, the as-calculated ones are too far off from the as-measured ones even though the former look somewhat similar to the latter in trends of variation. To drive a current of ~0.2 mA at 800 °C, e.g., only 0.2 V is expected on the basis of the continuity hypothesis, but in reality, a much higher force, 0.9 V, is required (see Fig. 1), indicating that the electronic conductivity of the bilayer is much more suppressed than expected on the basis of the continuity hypothesis (see Fig. 2). Obviously, Eq. (12) or Eq. (13) that is based on the continuity hypothesis fails in predicting correctly the chemical potential distribution under electric tension in ion-blocking condition in particular. It is, therefore, suggested that the continuity hypothesis may not necessarily be true.

IV. NEW HYPOTHESIS INTERFACIAL DISCONTINUITY

We hereby hypothesize that there will be, for some reasons, a discontinuity of oxygen potential at the interface between the two end-member electrolytes or a continuous drop across a very thin interfacial layer or interphase δ with a thickness L_δ, see Fig. 3(b). Letting μ'_O and μ''_O denote the oxygen chemical potential at the GDC/δ and δ/YSZ interface, respectively, Eq. (9) should then be modified to include the third term I_δ and, hence, Eq. (10) to include the corresponding term with oxygen potential bounds modified accordingly or

$$\frac{I}{A} = \frac{-1}{2F(L_C - L_\delta/2)}\int_{\mu'_O}^{\mu'_O}\sigma_{e,C}d\mu_O = \frac{-1}{2FL_\delta}\int_{\mu'_O}^{\mu''_O}\sigma_{e,\delta}d\mu_O = \frac{-1}{2F(L_Z - L_\delta/2)}\int_{\mu''_O}^{\mu''_O}\sigma_{e,Z}d\mu_O \quad . \quad (14)$$

Assuming $L_\delta << L_C$, L_Z, the first and third integral in Eq. (14) will take the same form as in Eqs. (11a) and (11b), respectively, but with $a^i_{O_2} = a'_{O_2}$ in the former and $a^i_{O_2} = a''_{O_2}$ in the latter.

From the as-measured I versus U in Fig. 1, one can now determine $a^i_{O_2} = a'_{O_2}$ via Eq. (11a) and $a^i_{O_2} = a''_{O_2}$ via Eq. (11b) again using the materials parameters in Table I. The results at the three temperatures are shown in Fig. 4.

It is seen that a great part of the overall oxygen potential drop ($\log a^I_{O_2} - \log a^{II}_{O_2}$) across the bilayer occurs over the δ-interphase ($\log a'_{O_2} - \log a''_{O_2}$). This interfacial drop tends to be arrested, and accordingly, the drop across the YSZ layer ($\log a''_{O_2} - \log a^{II}_{O_2}$) grows from ≈0 to maximum as σ_e of the bilayer approaches its minimum against a_{O_2} or the current I approaches its inflection point against U, see Figs. 1 and 2. Furthermore, the drop across the GDC layer is rendered negligibly small (i.e., $\log a^I_{O_2} - \log a'_{O_2} \to 0$), as temperature gets lower.

One may now estimate the mean area-specific resistance of each phase. Letting $<\sigma_{e,\phi}>$ and $\Delta_\phi \ln a_{O_2}$ denote

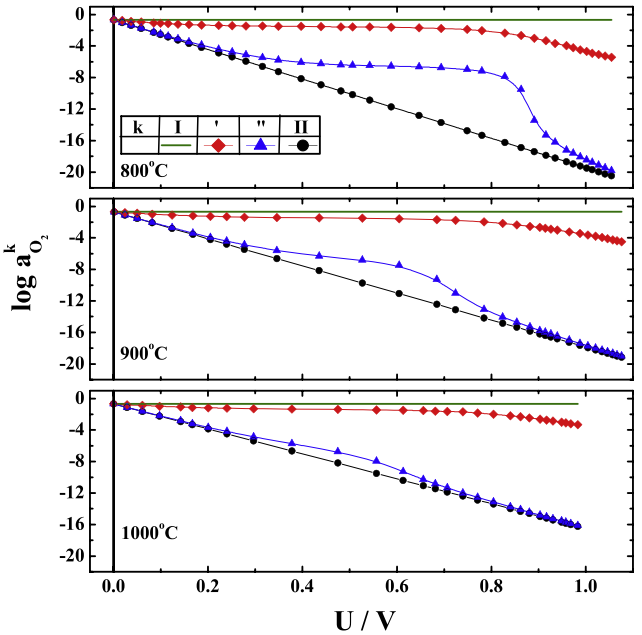


FIG. 4. As-calculated oxygen activities a'_{O_2} and a''_{O_2} across the interface of the $Ce_{0.9}Gd_{0.1}O_{1.95}/Zr_{0.84}Y_{0.16}O_{1.92}$ bilayer under electric tension U in ion-blocking condition at 800 °C (top), 900 °C (middle), and 1000 °C (bottom). GDC is on the reversible anode exposed to air ($a^I_{O_2} = 0.21$) and YSZ on the blocking cathode [$a^{II}_{O_2} = a^I_{O_2}\exp(-FU/RT)$].

https://doi.org/10.1557/jmr.2012.201 Published online by Cambridge University Press

the mean conductivity and oxygen activity drop across the phase ϕ (= C, δ, Z), respectively, the equation for each phase in Eq. (14) may be rewritten as

$$\frac{L_\phi}{<\sigma_{e,\phi}>} = -\frac{A}{I}\frac{RT}{4F}\Delta_\phi \ln a_{O_2} \quad , \qquad (15)$$

where the left-hand side corresponds to the mean area-specific resistance. The as-calculated $L_\phi/<\sigma_{e,\phi}>$ of the three constituent phases are shown in Fig. 5. One can clearly see that electron transfer is blocked mostly by the interface between GDC and YSZ or the interphase δ, rather than by the YSZ layer. The original idea of the bilayer electrolyte is to suppress the electronic conductivity of GDC by the thin complementary YSZ layer, which is electronically more resistive.[10] In this light, the present finding is interesting and suggestive as well.

The origin or nature of this electron-blocking interphase is at large at the moment. An extra potential drop or electronic resistance across a heterogeneous interface such as the phase boundary of present concern, however, is not totally unexpected: Different phases have, in general, different ionic and electronic transference numbers, thus each transference number must be discontinuous across a virgin interface. It is then unavoidable to have a nonvanishing divergence of partial ionic and electronic current, or $\nabla i_i \neq 0$, until the steady state where $\nabla i_i = 0$ is achieved under an electric field. It is well known[14,15] that wherever and whenever $\nabla i_i \neq 0$, there arises an electrochemical reaction to change the chemical composition or microstructure in the neighborhood of the singularity[14,15] in such a way that each partial current or flux is rendered continuous or $\nabla i_i = 0$ in the steady state. We believe that this will be the cause for the extra potential drop or electronic resistance across the interface of the bilayer of present concern. Additionally, one may also think of a narrow interdiffusion zone, insulating impurity phase (e.g., glass), or structural singularity at the heterogeneous interface as its origin.[16] Work is now underway to elucidate the detailed inner workings.

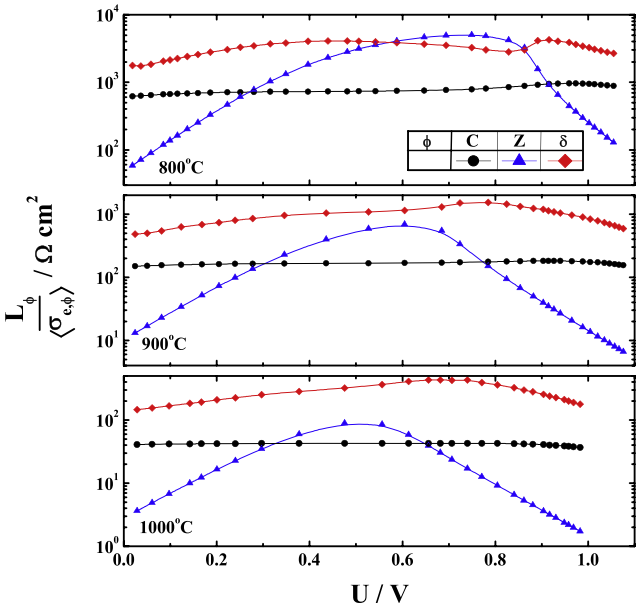


FIG. 5. Mean area-specific electronic resistances, $L_\phi/<\sigma_{e,\phi}>$ of GDC (ϕ = C), YSZ (ϕ = Z), and interface (ϕ = δ) in the bilayer electrolyte $Ce_{0.9}Gd_{0.1}O_{1.95}/Zr_{0.84}Y_{0.16}O_{1.92}$ versus applied voltage in Hebb–Wagner polarization cell at 800 °C (top), 900 °C (middle), and 1000 °C (bottom).

V. CONCLUSIONS

It is observed that the enhanced electronic resistance and extended electrolytic domain width of bilayer YSZ/GDC electrolytes appear to be mostly due to the phase boundary, rather than due to the electronically more resistive YSZ itself. This observation suggests that the widely accepted continuity hypothesis on steady-state chemical potential distribution across phase boundaries may break down for bilayer composite electrolytes under electric tension in ion-blocking condition. All the existing theories[1–6] dealing with the chemical potential distribution in a multilayer composite on the basis of this hypothesis, therefore, may not be always true depending on boundary conditions.

ACKNOWLEDGMENTS

This work was financially supported partially by the WCU project through National Research Foundation of Korea funded by the Ministry of Education, Science and Technology (R31-2008-000-10075-0) and partially by the Seoul R&D Program (CS070157).

REFERENCES

1. N.S. Choudhury and J.W. Patterson: Steady-state chemical potential profiles in solid electrolytes. *J. Electrochem. Soc.* **117**, 1348 (1970).
2. A.V. Virkar: Theoretical analysis of solid oxide fuel cells with two-layer, composite electrolytes: Electrolyte stability. *J. Electrochem. Soc.* **138**, 1481 (1991).
3. F.M.B. Marques and L.M. Navarro: Performance of double layer electrolyte cells Part I: Model behavior. *Solid State Ionics* **90**, 183 (1996).
4. S. Yuan and U. Pal: Analytic solution for charge transport and chemical-potential variation in single-layer and multilayer devices of different mixed-conducting oxides. *J. Electrochem. Soc.* **143**, 3214 (1996).
5. E.D. Wachsman, P. Jayaweera, N. Jiang, D.M. Lowe, and B.G. Pound: Stable high conductivity ceria/bismuth oxide bilayered electrolytes. *J. Electrochem. Soc.* **144**, 233 (1997).
6. S.H. Chan, J.J. Chen, and K.A. Khor: A simple bilayer electrolyte model for solid oxide fuel cells. *Solid State Ionics* **158**, 29 (2003).
7. R. Singh and K.T. Jacob: Calculation of the oxygen potential profile across solid-state electrochemical cells. *J. Appl. Electrochem.* **33**, 571 (2003).
8. T. Jacobsen and M. Mogensen: The course of oxygen partial pressure and electric potentials across an oxide electrolyte cell. *ECS Trans.* **13**, 259 (2008).

https://doi.org/10.1557/jmr.2012.201 Published online by Cambridge University Press

9. C. Wagner: On the electromotive force of the cell: Ag|AgI|Ag2S|Pt (+S). *Z. Elektrochem. Angew. Phys. Chem.* **40**, 364 (1934).
10. T-H. Kwon, T. Lee, and H-I. Yoo: Partial electronic conductivity and electrolytic domain of bilayer electrolyte $Zr_{0.84}Y_{0.16}O_{1.92}$/ $Ce_{0.9}Gd_{0.1}O_{1.95}$. *Solid State Ionics* **195**, 25 (2011).
11. J-H. Park and R.N. Blumenthal: Electronic transport in 8 mol percent Y_2O_3-ZrO_2. *J. Electrochem. Soc.* **136**, 2867 (1989).
12. S-H. Park: Tailoring of electrolytic domain of ceria-based electrolytes with electron traps. Ph.D. Thesis, Seoul National University, Seoul, Korea, 2008.
13. K-R. Lee, J-H. Lee, and H-I. Yoo: Reassessment of conventional polarization technique to measure partial electronic conductivity of electrolytes. *Solid State Ionics* **181**, 724 (2010).
14. H. Schmalzried: *Chemical Kinetics of Solids* (VCH, Weinheim, Germany, 1995); pp. 221–222.
15. H-I. Yoo and K-C. Lee: Microstructural changes in a polycrystalline, semiconducting oxide under DC electric fields. *J. Electrochem. Soc.* **145**, 4243 (1998).
16. H. Yokokawa: Private discussion.

https://doi.org/10.1557/jmr.2012.201 Published online by Cambridge University Press